

## Author's Response

Technical comments from editor:

1. Line 19. ... roles of the oxidation of volatile organic compounds (VOC).  
Response: corrected in line 19 in the new version, and the abbreviation of VOCs was added.
2. Lines 23, 24, 167, 168 and others. Use three significant numbers. The accuracy of the analytical methods used is not so high to use four significant numbers.  
Response: corrected in the new version, the significant number were limited to 2 significant numbers for the sources apportionment result, as seen in line 23, line 24, line 168, and line 169 in the new version.
3. Lines 28, 44 and others. ...of iron (Fe) and...  
Response: corrected in line 28 and line 45, and the "Iron" was corrected as "iron".
4. Line 37, A phrase of "could cause the coating thickness of black carbon" is not clear. It needs a rephrase.  
Response: the phrase was reorganized as "OH-initiated oxidation of m-xylene was found to cause the coating thickness of black carbon, which further induced the increase of particle size (1.5 to 10.4 times) and effective density (from 0.43 to 1.45 g cm<sup>-3</sup>)", as seen in line 38-40 in new version.
5. Line 56. Co-existent heterogenous.  
Response: corrected, line 57 in the new version.
6. Line 88. ...local time (LT) and..  
Response: corrected, line 89 in the new version.
7. Line 122, 155, 213, 280, 282, 289, 315, 316 and others. Add a space in between references and other places. ...5% (Ho et al., 2017; Ho et al., 2018).  
Response: corrected, line 66, line 68, line 183, line 214, line 280, line 282, line 289, line 315 and line 316.
8. Line 132. ...mixing ratio of the...  
Response: corrected, line 133 in the new version.
9. Line 136. ..., the levels of aromatics were...  
Response: corrected, line 137 in the new version.
10. Line 160. ...was a dominant source of...  
Response: corrected, line 161 in the new version.

11. line 179. use a superscript for ug m-3.  
Response: corrected, line 180 in the new version.
12. Line 196. Benzene  
Response: corrected, line 197 in the new version.
13. Line 220. ..., levels of ambient VOCs....  
Response: corrected, line 221 in the new version.
14. Line 238. Remove “And”.  
Response: corrected, line 239 in the new version.
15. Line 241. ...rush hours...  
Response: corrected, line 241 in the new version.
16. Line 250. ...relatively high..  
Response: corrected, line 250 in the new version.
17. Line 256. ...relatively active VOCs..  
Response: corrected, line 256 in the new version.
18. Line 257. ..would be aged with..  
Response: corrected, line 257 in the new version.
19. Line 263. ...of the VOC isomerides were...  
Response: corrected, line 263 in the new version.
20. Line 294. X/E ratios were..  
Response: corrected, line 294 in the new version.
21. Line 326. OC/EC ratios  
Response: corrected, line 326-328.
22. Line 327. In addition, the OC/EC ratios were reported...  
Response: corrected, line 326-328 in the new version.
23. Line 333. Summary and Conclusion  
Response: corrected.
24. Figures 5 and 6. Use a capital for Proportion of ..., and Fraction (%).lt.  
Response: corrected.

# Origin and Transformation of Ambient VOCs during a Dust-to-Haze Episode in Northwest China

Yonggang Xue<sup>1,2,3,4</sup>, Yu Huang<sup>1,2,3,4\*</sup>, Steven Sai Hang Ho<sup>1,2,5</sup>, Long Chen<sup>1,2,3,4</sup>, Liqin Wang<sup>1,2,3,4</sup>, Shuncheng Lee<sup>6</sup>, Junji Cao<sup>1,2,3,4\*</sup>,

<sup>1</sup>Key Lab of Aerosol Chemistry & Physics, Institute of Earth Environment, Chinese Academy of Sciences, Xi'an 710061, China

<sup>2</sup>State Key Lab of Loess and Quaternary Geology (SKLLQG), Institute of Earth Environment, Chinese Academy of Sciences, Xi'an 710061, China

<sup>3</sup>Shaanxi Key Laboratory of Atmospheric and Haze-fog Pollution Prevention, Institute of Earth Environment, Chinese Academy of Sciences, Xi'an 710061, China

<sup>4</sup>CAS Center for Excellence in Quaternary Science and Global Change, Xi'an, 710061, China.

<sup>5</sup>Division of Atmospheric Sciences, Desert Research Institute, Reno, Nevada, USA

<sup>6</sup>Department of Civil and Environmental Engineering, The Hong Kong Polytechnic University, Hung Hom, Hong Kong, China

Correspondence to: Yu Huang ([huangyu@ieecas.cn](mailto:huangyu@ieecas.cn))

Junji Cao ( [cao@loess.llqg.ac.cn](mailto:cao@loess.llqg.ac.cn) )

**Abstract.** High contribution of secondary organic aerosol to the loading of fine particle pollution in China highlights the roles of volatile organic compounds (VOCs) oxidation. Therein, particulate active metallic oxides in dust, like TiO<sub>2</sub> and Fe ions, were proposed to influence the photochemical reactions of ambient VOCs. A case study was conducted at an urban site in Xi'an, northwestern China, to investigate the origin and transformation of VOCs during a windblown dust-to-haze pollution episode, and the assumption that dust would enhance the oxidation of VOCs was verified. Local vehicle exhaust (25%) and biomass burning (18%) were found to be the two largest contributors to ambient VOCs. In the dust pollution period, sharp decrease of VOCs loading and aging of their components were observed. Simultaneously, the secondary oxygenated VOCs fraction (i.e., methylglyoxal) increased. Source strength, physical dispersion, and regional transport were eliminated from the major factor for the variation of ambient VOCs. In another aspect, about 2 and 3 times increase of the loading of iron (Fe) and titanium (Ti) was found in the airborne particle, together with fast decrease of trans-/cis-2-butene ratios which demonstrated that dust can accelerate the oxidation of ambient VOCs and formation of SOA precursors.

## 33 **1 Introduction**

34 Secondary aerosols are important components of fine particles in China, which could contribute to about  
35 30 to 77 percent of PM<sub>2.5</sub> loading, therein, secondary organic aerosols (SOA) take about half of the  
36 loading (Huang et al., 2014). Guo et al. (2014) believed that gaseous emissions of volatile organic  
37 compounds (VOCs) and nitrogen oxides (NO<sub>x</sub>) were responsible for the large secondary PM formation.  
38 OH-initiated oxidation of m-xylene was found to cause the coating thickness of black carbon, which  
39 further induced the increase of particle size (1.5 to 10.4 times) and effective density (from 0.43 to 1.45 g  
40 cm<sup>-3</sup>) (Guo et al., 2016).

41 Solid-gas heterogeneous reactions would cause the transformation of gaseous pollutants and change  
42 the property of particles (Zhang et al., 2000; Zhang et al., 2003; He et al., 2014). Recently, the oxidation  
43 of organic and inorganic gas on particles surface through the transitional-metal-catalyzed chain reaction  
44 was frequently found to play important roles on the transformation of ambient gas pollutants (Chu et al.,  
45 2019). Mineral dust is the most important sources of the transitional-metal, like iron (Fe) and titanium  
46 (Ti), in the natural environment (Chen et al., 2012). In addition, mineral dust is one kind of the most  
47 abundant components of the global airborne PM, and about 1600 to 2000 Tg of mineral dust is  
48 transformed to aerosols annually from major deserts (Ginoux et al., 2001). Furthermore, the surface of  
49 mineral dust provides plenty of reactive sites for multiple atmospheric trace gas reactions (Cwiertny et al.,  
50 2008). As a result, dust was viewed to serve as catalyst for reactive gas, and modify the photochemical  
51 processes (Dentener et al., 1996; Dickerson et al., 1997).

52 With the controlled experiment of sulfate formation on mineral dust, Zhang et al. (2019) found that  
53 under appropriate humidity and particle acidity, surface transitional-metal-catalyzed chain reaction  
54 together with nitrate would highly accelerate the sulfate's formation on the surface of mineral dust  
55 (Zhang et al., 2019). In another aspect, gas-solid heterogeneous photochemical reactions of organic  
56 compounds were also reported on the illuminated surface of semiconductor metal oxides in the natural  
57 environment, in particular TiO<sub>2</sub> (Chen et al., 2012). Co-existent heterogeneous photochemical reactions  
58 of SO<sub>2</sub>, NO<sub>2</sub> and VOCs on the surface of mineral dust were investigated in recent years. Both synergistic  
59 and suppress effects of VOCs on the formation of sulfate were found, which indicated the competition of  
60 reactive oxygen species and active sites between VOCs and inorganic gas pollutants (Chu et al., 2019;

61 Song et al., 2019). In addition, oxidized products, like formate and acetate species, were observed in the  
62 co-existence reaction, which highlight the possibility of further oxidation of VOCs on the mineral dust  
63 (He et al., 2014). In northwestern China, dust from both local sources and long-range transport is one of  
64 the most important components of particulate matter of  $< 2.5 \mu\text{m}$  in diameter ( $\text{PM}_{2.5}$ ) (Huang et al., 2014).  
65 Xi'an has a population of  $\sim 8$  million (Feng et al., 2016). The sharp increase of vehicles and other human  
66 activities has led to high emissions of VOCs and  $\text{NO}_x$  (Li et al., 2017). Observations showing  
67 simultaneous high dust loading and elevated VOCs and  $\text{NO}_x$  concentrations suggest possible impacts  
68 from heterogeneous reaction on dust particles (Huang et al., 2014; Li et al., 2017). The present study was  
69 conducted to investigate the origin and transformation of ambient VOCs with severe dust-to-haze episode  
70 in winter. The transformation and the related chemical processing of ambient VOCs and the related  
71 changes in the composition of  $\text{PM}_{2.5}$  were studied, within typical windblown dust-to-haze episodes. The  
72 potential pathway of VOCs oxidation in the windblown dust-to-haze formation process was explored.

## 73 **2 Materials and Methods**

### 74 **2.1 Sampling site**

75 An observation site (E 109°00'7", N 34°13'22") managed by Xi'an Jiaotong University was used in  
76 this study (Figure 1). All sampling equipment was deployed on the rooftop of a 15-m tall academic  
77 building. No obvious stationary pollution sources were found nearby, and the location can be considered  
78 as a typical urban location in Xi'an (Zhang et al., 2015a).

### 79 **2.2 Field Sampling**

80 Severe dust-to-haze episode was observed in Xi'an and the surrounding areas from 8 November to 12  
81 November in 2016, and samples was continuously collected during this period to investigate the chemical  
82 compositions of both VOCs and fine PM. A total of 57 non-methane VOCs species (i.e.,  $\text{C}_2\text{-C}_{12}$   
83 saturated and unsaturated aliphatic and aromatic VOCs) were sampled hourly into offline multi-bed  
84 adsorbent tubes; the measured 57 VOCs were defined as  $\text{VOC}_{\text{PAMS}}$ . The loaded tubes were analyzed  
85 using a thermal desorption and gas chromatography/mass spectrometry (TD-GC/MS) method. In  
86 previous developmental work, humidity and temperature during sampling were found to impact  
87 significantly on the analyses; for this study, all sample collections were made under optimized conditions

88 (Ho et al., 2017; Ho et al., 2018). Sixteen airborne carbonyls (including mono- and dicarbonyls) were  
89 collected over diurnal cycles (i.e., 20:00–08:00 local time (LT) and 08:00–20:00 LT) by  
90 2,4-dinitrophenylhydrazine (DNPH) coated-cartridges. Detailed sampling and analytical procedures for  
91 VOCs and carbonyls can be found in previous publication (Ho et al., 2017; Dai et al., 2012).

92 PM<sub>2.5</sub> filter samples were sampled with mini-volume samplers (Model Mini-Vol, Air Metrics Co.,  
93 Oregon, USA) by a flow rate of 5 L min<sup>-1</sup> (Cao et al., 2005). Fine PM was sampled by 47-mm quartz  
94 microfiber filters (Whatman QM/A, Maidstone, UK), and the filters were pre-heated at 900°C for 3-h  
95 before sampling. The loaded filters were transferred into clean polystyrene petri dishes and stored in a  
96 freezer.

### 97 **2.3 Chemical Analyses**

98 Analytical procedures for VOC analysis have been described previously (Ho et al., 2017). In brief, the  
99 analytes in the adsorbent tubes were firstly desorbed in a thermal desorption unit (Series 2 UNITY-xr  
100 system with ULTRA-xr, Markes International, Ltd., UK) coupled to a GC/MS (7890A/5977B, Agilent  
101 Technologies, Santa Clara, CA, USA). The loaded tube was transferred into the TD unit and blown with  
102 ultra-high purity He gas. The targeted VOCs were desorbed at 330°C within 8 mins, and then refocused  
103 onto a cryogenic-trap (U-T1703P-2S, Markes) at -15°C. The targeted VOCs were transferred to a cold  
104 GC capillary column head (Rtx®-1, 105 m × 0.25 mm × 1 mm film thickness, Restek Corporation, USA)  
105 at -45°C. The chromatographic condition could be found in our previous work (Ho et al., 2017).

106 For carbonyl compounds, the DNPH cartridges were firstly eluted with acetonitrile (HPLC/GCMS  
107 grade, J & K Scientific Ltd., Ontario, Canada) (Dai et al., 2012). The extracts were analyzed with a  
108 typical high-pressure liquid chromatography (HPLC) system (Series 1200; Agilent Technologies)  
109 equipped with photodiode array detector. The column was matched with a 4.6 × 250 mm Spheri-5 ODS 5  
110 μm C-18 reversed-phase column (Perkin-Elmer Corp., Norwalk, CT) (Dai et al., 2012; Ho et al., 2011).

111 The particulate organic carbon (OC) and elementary carbon (EC) were analyzed with a DRI model  
112 2001 carbon analyzer (Atmoslytic, Inc., Calabasas, CA, USA) (Chow et al., 2007; Chow et al., 1993).  
113 Anions (Cl<sup>-</sup>, NO<sub>3</sub><sup>-</sup>, and SO<sub>4</sub><sup>2-</sup>) and cations (Na<sup>+</sup>, NH<sub>4</sub><sup>+</sup>, K<sup>+</sup>, Mg<sup>2+</sup>, and Ca<sup>2+</sup>) in particles were determined  
114 in aqueous extracts of the sample filters. Detailed extraction and analytical procedures were presented in

115 a previous publication (Zhang et al., 2011). The abundances of 25 particulate elements (Na, Mg, Al, Si,  
116 S, Cl, K, Ca, Sc, Ti, V, Cr, Mn, Fe, Co, Ni, Cu, As, Se, Br, Sr, Ba, Pb, Ga, Zn) were measured by  
117 energy dispersive x-ray fluorescence (ED-XRF) spectrometry (Epsilon 4 ED-XRF, PAN alytical B.V.,  
118 the Netherlands). The X-ray source was matched with a metal-ceramic X-ray tube with a Rh and Ag  
119 anode, and X-ray source was operated at a maximum current of 3mA, and the maximum accelerating  
120 voltage of 50kV (maximum power 15W).

## 121 **2.4 Quality Control**

122 The Minimum detection limits (MDLs) of the VOCs were in the range of 0.003–0.042 ppbv with a 3 L  
123 sampling volume (Table S1). The measurement precision at 2 ppbv was  $\leq 5\%$  (Ho et al., 2017; Ho et al.,  
124 2018). Three field blank samples were collected within each sampling day, and they were analyzed using  
125 the same procedures as those for the ambient air samples. Most target compounds were not detected in  
126 the field blanks, and propylene, benzene, and toluene were below their MDLs ( $< 0.23$  g per tube and  $<$   
127 10% of the arithmetic mean of ambient samples). No breakthrough ( $\sim 0\%$ ) was observed for VOC<sub>SPAMS</sub>  
128 except for C<sub>2</sub>–C<sub>3</sub> hydrocarbons, which were  $< 10\%$  when the air temperature was  $> 30^\circ\text{C}$ . The MDLs for  
129 the carbonyl target compounds were between 0.009 to 0.067 ppbv at a sampling volume of 3.6 m<sup>3</sup>.  
130 Negligible breakthrough ( $< 5\%$ ) was found under the sampling conditions and flow rates in the field.

## 131 **3. Results and Discussion**

### 132 **3.1 Origins of ambient VOCs during Dust and Fine-particle Pollution Events**

133 In the present study, mixing ratio of the sum of non-methane hydrocarbon was  $36.0 \pm 15.7$ ppbv, which  
134 was lower comparing to that in Beijing and Guangzhou with values of 51.0 and 47.8 ppbv, respectively  
135 (Ho et al., 2004; Liu et al., 2008b). Similar levels of alkenes were seen at the cities of Beijing (9.4 ppbv)  
136 and Guangzhou (8.2 ppbv) comparing to that in the present study (9.2 ppbv, Table S2, Ho et al., 2004;  
137 Liu et al., 2008b). Unexpectedly, the levels of aromatics were slightly higher in Xi'an (10.3 ppbv) than  
138 that in Beijing (9.6 ppbv), and 50% higher than that in Guangzhou (6.8 ppbv, Shao et al., 2009; Zou et al.,  
139 2015). Therein, ethylene, ethane, toluene, iso-pentane, propane, n-butane, iso-butane, propylene,  
140 n-pentane, and benzene were the most 10 abundant VOC<sub>SPAMS</sub>. The high fractions of these markers  
141 reflect strong emissions from traffic and coal combustion or from biomass burning (Liu et al., 2008a; Ho

142 et al., 2009; Huang et al., 2015; Fan et al., 2014; Zhang et al., 2015c). Previous studies found higher  
143 contributions of non-fossil sources to carbonaceous aerosols in Xi'an, as compared with Beijing (Ni et al.,  
144 2018). Generally, non-fossil emissions mainly originate from biomass burning (Ni et al., 2018), and the  
145 higher contribution of non-fossil sources to carbonaceous in Xi'an would indicate remarkable biomass  
146 burning activities exist in Xi'an and the surrounding areas (Huang et al., 2014; Xu et al., 2016).

147 Receptor models and correlations between individual VOCs have been used for source assessments. In  
148 this study, significant correlation ( $R^2=0.62$ ,  $p<0.05$ , slope of 1.59) was found for a least-squares  
149 regression between toluene and benzene (Figure S1). The ratio of toluene to benzene (T/B) ratio has been  
150 shown to different among combustion sources; for example, Liu et al. (2006) reported T/B ratios of  
151 1.5-2.0 in gasoline-related emissions collected in a tunnel. In contrast, T/B ratios ranged from 0.23-0.68  
152 and 0.13-0.71 for biomass burning and coal combustion, respectively (Zhang et al., 2015c). The T/B  
153 ratios in our samples ( $R^2=0.62$ ,  $p<0.05$ , slope of 1.59) implied a strong impact from traffic on the  
154 ambient VOCs in Xi'an. Significant correlations ( $p<0.05$ ) were observed among  $C_3$ - $C_5$  alkanes, with  
155 propane versus n-butane ( $R^2=0.75$ , slope=0.91), n-pentane versus iso-pentane ( $R^2=0.85$ , slope=0.35), and  
156 trans-2-butene versus cis-2-butene ( $R^2=0.99$ , slope=0.84) (Figure S1). The observed ratio of propane to  
157 n-butane in Xi'an was 1.1, which is close to that (1.36) observed in the tunnel study cited above (Liu et  
158 al., 2008). High loadings of n-pentane and iso-pentane are indicative of unburned vehicular emissions,  
159 and Liu et al., (2008) reported a ratio of iso-pentane/n-pentane of 3 in tunnel air, which is consistent with  
160 the slope of 2.85 found in the present study. The ratios of T/B, trans-/cis-2-butene, propane/n-butane and  
161 n-pentane/iso-pentane indicated that gasoline emission was a dominated source of ambient VOCs, and  
162 the source apportionment by PMF model result, and the detail description of source apportionment will  
163 be carried out in the following section.

164 PMF model was used to identify the major pollution sources: the data input to the model were the  
165 mixing ratios and uncertainties in the VOCs mixing ratios for all valid samples collected during the study.  
166 Five sources were identified (Figure S2), and the detail process of source apportionment were given in  
167 the supporting information. Biomass burning and gasoline exhaust were the two most significant  
168 pollution sources, contributing 25% and 18%, respectively. The combustion of LPG and CNG (25%),  
169 diesel exhaust (15%), coal combustion (17%) also were found to be important sources of ambient VOCs  
170 (Figure S2). Biomass is commonly used for heating and cooking in rural areas of the basin in winter due  
171 to its low cost compared with natural gas and electricity. Consistent with our results, previous studies



172 found high contribution of biomass burning and gasoline exhaust to the organic aerosol in Guanzhong  
173 Basin (Cao et al., 2005).

174 Clear air conditions occurred at the beginning of the sampling period, but severe dust and fine-particle  
175 pollution events were observed afterward. The high dust event was defined by loading of particulate  
176 matter  $\leq 10 \mu\text{m}$  in aerodynamic diameter ( $\text{PM}_{10}$ ) between  $300$  and  $500 \mu\text{g m}^{-3}$ , and these conditions  
177 occurred from 12:00 LT on 9 November to 13:00 LT on 10 November. The abatement of dust before the  
178 fine particle pollution event is referred to as the transition period (i.e.,  $\text{PM}_{10} < 300 \mu\text{g m}^{-3}$  and  $\text{PM}_{2.5} <$   
179  $100 \mu\text{g m}^{-3}$ ). The loading of  $\text{PM}_{2.5}$  subsequently increased, and heavy fine particle pollution ( $\text{PM}_{2.5} > 100$   
180  $\mu\text{g m}^{-3}$ ) occurred after 18:00 LT on 11 November.

181 Ratios of individual VOCs can be used to identify the origins of the compounds and to study  
182 atmospheric aging processes due to the special composition of VOCs in a typical source and the different  
183 lifetime of VOCs species (Xue et al., 2017; Zhang et al., 2015c). In addition, influences from  
184 meteorological variation and atmospheric transport also need to be considered when the potential sources  
185 of the compounds in ambient air are characterized. To investigate the impacts of air mass transport on  
186 VOCs concentrations, we calculated air-mass back trajectories using the NOAA HYSPLIT model for the  
187 dust event (Figure S4a) and for the fine-particle pollution episode (Figure S4b). The trajectories were  
188 calculated at an arrival height of 500 m above ground at the observation site. In view of the short  
189 atmospheric lifetimes of VOCs (for example, isoprene,  $\sim 1.4$  h; propylene,  $\sim 5.3$  h; toluene, 2.1 d)  
190 (Atkinson and Arey, 2003), 24-h back trajectories were used for this assessment.

191 Clear different air masses back trajectories and VOCs ratios were observed between dust pollution and  
192 haze pollution periods. From 9 November to 10 November (in dust pollution period), the air mass  
193 reaching Xi'an passed over areas to the west of the city (i.e., Gansu Province and Ningxia Autonomous  
194 Region) through long range transport; after 11 November (formation of haze), the transport of air mass  
195 was mainly limited to areas around southern Xi'an. Differences in the chemical compositions of ambient  
196 VOCs in the dusty versus in the haze event can clearly be seen (Figure 2) in the ratios of toluene to  
197 benzene (T/B, Toluene,  $K_{\text{OH}} 5.96 \times 10^{-12} \text{ cm}^3 \text{ molecule}^{-1} \text{ s}^{-1}$ , Benzene,  $K_{\text{OH}} 1.22 \times 10^{-12} \text{ cm}^3 \text{ molecule}^{-1}$   
198  $\text{s}^{-1}$ ) and m, p-xylene to ethylbenzene (X/E, m-xylene,  $K_{\text{OH}} 2.30 \times 10^{-11} \text{ cm}^3 \text{ molecule}^{-1} \text{ s}^{-1}$ , p-xylene,  $K_{\text{OH}}$   
199  $1.43 \times 10^{-11} \text{ cm}^3 \text{ molecule}^{-1} \text{ s}^{-1}$ , ethylbenzene,  $K_{\text{OH}} 7.00 \times 10^{-12} \text{ cm}^3 \text{ molecule}^{-1} \text{ s}^{-1}$ ). During the clear and  
200 dusty periods, the T/B and X/E ratios varied significantly with time of day; that is, the highest values for  
201 T/B (4.5–9.0) and X/E (0.98–1.05) were seen during rush hour (07:00–09:00 LT and 17:00–19:00 LT),

202 while the lowest values (0.50–1.95 for T/B, and 0.89–0.96 for X/E) occurred in the early afternoon (i.e.,  
203 14:00–15:00 LT). The timings of the high T/B and X/E ratios suggest that fresh emissions from local  
204 traffic were the major source for the ambient VOCs, and this implies that long-range transport did not  
205 have a strong impact on the ambient VOCs during the clear or dusty parts of the study (Ho et al., 2004;  
206 Liu et al., 2008a). While during the transitional and fine PM pollution period, both T/B and X/E varied  
207 but at relatively lower values compared with the earlier parts of the study (T/B,  $3.33\pm 1.97$ ,  $2.21\pm 0.86$ ,  
208  $1.91\pm 0.74$ ,  $2.01\pm 0.56$  in clear, dust, transitional and fine particle pollution periods, respectively; X/E,  
209  $1.00\pm 0.05$ ,  $1.05\pm 0.12$ ,  $0.93\pm 0.17$ ,  $0.95\pm 0.13$  in clear, dust, transitional and fine particle pollution periods,  
210 respectively). These synchronous lower values of T/B and X/B in transitional and fine particle pollution  
211 periods were indicative of aged air masses (Zhang et al., 2015c; Xue et al., 2017; Warneke et al., 2013).

212 Variations in the air mass transport pathway, and T/B or X/E during different sampling periods (clear,  
213 dust, transitional, fine particle pollution) confirmed that ambient VOCs were fresh in the clear and dust  
214 periods, but relatively aged during the transitional and fine particle pollution periods (Zhang et al., 2015c;  
215 Xue et al., 2017; Warneke et al., 2013). This indicates that the long-range transport of air mass had a  
216 relatively weak influence on the ambient VOCs even during the high dust period. Otherwise,  
217 composition of ambient VOCs should be relative aged due to long exposure time with dust transport.  
218 Indeed, emissions from local vehicular exhausts and biomass burning in Xi'an and the surrounding areas  
219 were the main contributors to ambient VOCs throughout our study.

### 220 **3.2 Transformation of VOCs between Dust and Fine Particle Events**

221 With the shading of dust, [levels](#) of ambient VOCs decreased with time, and the low concentrations (8.3  
222 to 33.9 ppbv) were observed from 13:00 LT on 10 November and 01:00 LT on 11 November (Figure 3).  
223 During the fine particle pollution period (12–13 November), the  $\Sigma \text{VOC}_{\text{SPAMS}}$  increased, reaching an  
224 average of 38.0 ppbv in the last 24 h, compared with 19.0 ppbv in the transitional period and 21.5 ppbv  
225 in the first 12 h of the fine particle pollution episode (Figure 3). This buildup of VOCs can be explained  
226 by weak dispersion and relatively shallow boundary layers (400–1000 m) during the event (Figure 3). In  
227 addition, during this transition period, much lower ratios of T/B and X/E were observed in comparison  
228 with those in other periods (as mentioned in the part 3.1.2). We propose the possibility that windblown  
229 dust which include sustainable  $\text{TiO}_2$  can influence the atmospheric photochemistry of VOCs, which  
230 would accelerate the oxidation of ambient VOCs (Chu et al. 2019; Nie et al., 2014).

231 While changes in the emission sources and their strengths, physical dispersion, regional transport, and  
232 aging of air masses all could affect VOC levels and composition (Xue et al., 2013; Xue et al., 2017). As a  
233 result, to evaluate aging of ambient VOCs in different period, the impact of dust on the transform of  
234 ambient VOCs, and the relative processes, the mentioned factors should be fully considered.

235 To evaluate the impact of sources types on the variation of VOCs in the dust-to-haze episode, diurnal  
236 variation of VOCs was depicted. During the clear and dusty periods—and similar to the trends in T/B  
237 and X/E ratios—peaks in  $\Sigma \text{VOC}_{\text{SPAMS}}$  were seen from 17:00 to 20:00 LT and from 09:00 to 12:00 LT  
238 (Figure 3), which highlighted the impacts of local traffic emission (Liu et al., 2008a; Huang et al., 2015).  
239 1,3-Butadiene is often used as marker of gasoline-powered motor vehicles (Huang et al., 2015), while  
240 ethane is key chemical marker for biomass and coal combustion (Liu et al., 2008a). Time series plots of  
241 1,3-butadiene and ethane (Figure S5) show that peaks in 1,3-butadiene mostly occurred during **rush hours**,  
242 while higher concentrations of ethane were seen during the night. These results support the conclusions  
243 that there were strong impacts from gasoline-powered motor vehicles in the daytime and from biomass  
244 burning or coal combustion for heating at night. In addition, winter heating activities was relatively  
245 active because of low temperatures during the transitional period, and this limited the possibility of  
246 reduced emission amounts. Hence the variations of sources strength was eliminated from the major factor  
247 caused the extremely low concentration and relative aged composition of ambient VOCs.

248 Variation of physical dispersion was also eliminated. With the shading of dust transport, shallow  
249 boundary layers were observed in the transitional period. For the clear and dust transport period, the  
250 boundary layer between 08:00 to 14:00 was relatively **high** (1150–1500 m). In contrast, the boundary  
251 layer height decreased sharply to < 800 m on 11 November in transitional period. This limited the  
252 possibility that diffusion caused the sharp decrease of ambient VOCs in the transitional period.

253 Significant impact of air mass input was eliminated. Input of air mass would certainly cause the  
254 variations of VOCs' composition and loading (Xue et al., 2014). In the present study, long range  
255 transport of air masses had limited impacts on the characteristic of ambient VOCs during the sampling  
256 period. In another aspect, **relatively** active VOCs would be firstly degraded, hence composition of  
257 ambient VOCs would be **aged** with long range transport (Ho et al., 2009; Xue et al., 2017). While in the  
258 present study, as mentioned above, composition of ambient VOCs was relative fresh under long range  
259 transport of air mass (within dust transport). In contrast, VOCs composition was relatively aged under the  
260 air mass that limited with Xi'an and the surrounding area (transitional period). This phenomenon

261 indicated that regional transport cannot be the major factor inducing the relative aged composition and  
262 excess low loading of the ambient VOCs in the transitional period.

263 Synchronous changes of the VOCs [isomerides](#) were found in the windblown dust-to-haze episode,  
264 which supplied the evidence of the accelerated photochemistry reactions. In the present study, we  
265 found fast decrease of trans-/cis-2-butene ratio within dust transporting, which confirmed the accelerated  
266 photochemical reactions of ambient VOCs (Figure 4). Trans-2-butene and cis-2-butene are two  
267 isomerides that mostly emitted from same sources (Zheng et al., 2017; Zhang et al., 2015b). While  
268 trans-2-butene has higher photochemical reactions rate with OH radical in the atmosphere ( $k_{OH}$   
269  $6.40 \times 10^{-11} \text{ cm}^3 \text{ molecule}^{-1} \text{ s}^{-1}$ ) than cis-2-butene ( $k_{OH}$   $5.64 \times 10^{-11} \text{ cm}^3 \text{ molecule}^{-1} \text{ s}^{-1}$ ) (Perring et al.,  
270 2013), hence trans-/cis-2-butene ratio would decrease with the photochemical reactions (Zhang et al.,  
271 2015b). Firstly, relative higher trans-/cis-2-butene ratios were observed in the rush hours (evening rush  
272 hours 17:00-20:00, morning rush hours 07:00-10:00) (Figure 4), which indicated fresh emission from  
273 local traffic activities (Zhang et al., 2015b). In addition, sharp decrease of trans-/cis-2-butene ratio was  
274 observed from late half of windblown dust period to the end of transitional period (Figure 4). The quickly  
275 shrinking of trans-2-butene comparing to cis-2-butene in the dust pollution period indicated that  
276 oxidation of ambient VOCs was accelerated in the period with high loading of the suspending dust  
277 particles (Zhang et al., 2015b).

278 Significant increase of particulate active metals was found in dust pollution period, which further  
279 verified the promotion of dust on the heterogeneous reactions. Previous study found that mineral dust can  
280 affect the chemistry of the atmosphere by scavenging gaseous compounds (Zhang et al., 2000; Chen et al.,  
281 2012); it can also promote heterogeneous reactions of atmospheric substances, including VOCs, because  
282 the particle surfaces can provide sites for photo-catalytic reactions (Cwiertny et al., 2008; Ndour et al.,  
283 2009). In the present study, ferrum (Fe) and titanium (Ti) contents of the particulate increased  
284 significantly within the period with dust transport (Figure 5). In detail, content of Fe increased from  $19.3$   
285  $\mu\text{g m}^{-3}$  in clear days to  $40.8 \mu\text{g m}^{-3}$  in dust pollution days, and the content of Ti increased from  $0.92$  to  
286  $2.98 \mu\text{g m}^{-3}$ . Hence, huge increase of the Ti and Fe concentrations in particulate phase during the period  
287 of dust pollution days could possibly promote the gas-solid photochemical reaction of the ambient VOCs,  
288 which would reasonably ascribe the relative low level and aged composition of ambient VOCs in this  
289 period (Chu et al., 2019; He et al., 2014; Song et al., 2019).

290 **3.3 Variation of carbonyl compounds between dust to fine particle pollution periods: further**  
291 **formation oxygenated VOCs with aging of primary VOCs**

292 Aging of primary VOCs and formation of carbonyl compounds were observed synchronously, as the  
293 fine-particle pollution event developed (Figure 3; Figure 6a). As discussed above, relatively low T/B and  
294 X/E ratios were observed during the transitional and fine PM periods after the dust event (Part 3.2). In  
295 our study, the carbonyl levels increased after the clear and dusty periods, and the highest levels were seen  
296 during the fine particle pollution event (Figure 6a). Carbonyl compounds are produced from both the  
297 primary sources and form through secondary processes (Dai et al., 2012; Duan et al., 2012), and we  
298 found higher carbonyl concentrations during daytime than at night (Figure 6a). This is consistent with  
299 previous studies in Xi'an (Dai et al., 2012), which confirmed the secondary formation of carbonyl  
300 compound under sunlight illumination.

301 Methylglyoxal is generally considered to be a secondary species, while acetone is mainly from primary  
302 emissions; the ratio of acetone to methylglyoxal (A/M) has been used as an indicator of air mass aging  
303 (Dai et al., 2012; Liu et al., 2006). In the present study, A/M ranged from 12 to 14 during the clear and  
304 first half of dusty periods but then dropped sharply and stayed between 6 and 9 during the later parts of  
305 dust pollution period, transitional and the high PM event (Figure 6a). Increases in the abundances of  
306 carbonyl compounds and lower A/M ratios suggested relatively stronger aging of the air masses, this is  
307 further evidence of fast degradation of VOCs in the late half of the windblown dust event, and the  
308 primary VOCs were oxidized and served as precursors of SOA. In consequence, composition of particles  
309 changed with oxidation of ambient VOCs across the sampling periods.

310 **3.4 Variations of PM<sub>2.5</sub> Chemical Composition during Dusty and Fine PM Pollution Periods**

311 Significant variations of water-soluble inorganic ions, OC, and EC were observed diurnally and  
312 between dust and fine particle pollution events (Figure 6b, c). For instance, the concentrations of NO<sub>3</sub><sup>-</sup>  
313 were relatively high in the daytime, while K<sup>+</sup> and Cl<sup>-</sup> were more abundant at night. The diurnal cycles can  
314 be explained by the formation of secondary particles through photochemical processes during the  
315 daytime and by the impacts from biomass and coal burning for heating at night (Dai et al., 2012; Zhang  
316 et al., 2018; Cong et al., 2015). The concentrations of Ca<sup>2+</sup>, Mg<sup>2+</sup>, and Na<sup>+</sup>, which are typically associated  
317 with dust in inland areas (Wu et al., 2011), increased sharply during the dusty period, and then declined  
318 rapidly afterwards.

319 As discussed, the apparent contribution of VOCs to the formation of SOAs increased when the dusty  
320 conditions transitioned into a fine-particle pollution event. Temporal changes in the chemical  
321 composition of PM<sub>2.5</sub> are consistent with this suggestion. During the fine-particle pollution period, both  
322 the concentrations of secondary ions, particularly NO<sub>3</sub><sup>-</sup>, increased as the haze event developed. A similar  
323 trend was seen for OC (Figure 6b), and content of particulate OC increased from 11.1 μg m<sup>-3</sup> since dust  
324 event period to 47.1 μg m<sup>-3</sup> in the haze period. In another aspect, the ratio of OC/EC increased from 1.3 to  
325 4.9 in the dust-to-haze episode. The previous studies on the characterization of particles from traffic  
326 emission reported OC/EC ratios in the range of 0.28 to 0.92 in the diesel vehicles, and the OC/EC ratios  
327 were reported >2 in the gasoline vehicles (Cadle et al., 1999; Huang et al., 2006). In addition, the OC/EC  
328 ratios were reported in the range of 0.9 to 1.6 in the urban region in the city of Guangzhou (Tao et al.,  
329 2019). In the present study, the consistent increase of OC/EC would prove the formation of SOA in the  
330 dust-to-haze episode. Combined with the findings regarding the compositions of VOCs and PM<sub>2.5</sub>, these  
331 results indicate that the reactions of VOCs led to the formation of SOA, and in so doing contributed to  
332 the fine particle pollution.

#### 333 4. Summary and Conclusion

334 Comprehensive field work was carried out to investigate the origin and transform of VOCs within the  
335 dust-fine particles pollution periods in winter with the city of Xi'an. And the assumption of promotions  
336 of dust on the heterogeneous reactions of VOCs was further verified. Local vehicle exhaust and heating  
337 activities were found to be the most important sources of the ambient VOCs in Xi'an within winter,  
338 while long range transport air mass has limited impacts. Within the period of dust transport, loading of  
339 ambient VOCs decreased sharply from the late half period, and the lowest concentration was observed in  
340 the transitional period, in accordance with aging of primary VOCs. In addition, loading and proportion of  
341 secondary VOCs in gaseous phase and secondary ions and organic carbon in particulate phase increased  
342 with the aging of primary VOCs. Source strength, physical dispersion, and regional transport were  
343 eliminated from the major factor for the variation of the ambient VOCs. On another aspect, sharp  
344 increase of active metals concentrations (Ti and Fe) and fast decrease of trans-/cis-2-butene ratio were  
345 observed from the late half of dust transport period. In consequence, we conclude that windblown dust

346 might accelerate the gas-solid heterogeneous reactions of atmospheric VOCs, and further induced the  
347 formation of SOA precursors.

348

349 *Data availability.* All of the research data have been included in the supplement.

350

351 *Supplement.* The following information is provided in the Supplement: Sampling procedures, Chemical  
352 Analysis, Source characterization, Figure S1-S5, Table S1-S2.

353

354 *Author contributions.* YX designed the study. YX and YH wrote the paper. SH, JC and SL revised the  
355 manuscript, LC and LW analyzed the data. All authors reviewed and commented on the paper.

356

357 *Competing interests.* The authors declare that they have no conflict of interest.

358

359 *Acknowledgements.* This research was financially supported by the National Key Research and  
360 Development Program of China (Grant No. 2016YFA0203000), and the National Science Foundation of  
361 China (Grant No. 41701565, 21661132005, 41573138). Yu Huang was also supported by the “Hundred  
362 Talent Program” of the Chinese Academy of Sciences. The data used are listed in the supplements.

## 363 **References**

364 Atkinson, R., and Arey, J.: Atmospheric Degradation of Volatile Organic Compounds, *Chem. Rev.*, 103,  
365 4605-4638, <https://doi.10.1021/cr0206420>, 2003.

366 Cadle SH, Mulawa PA, Hunsanger EC, Nelson K, Ragazzi RA, Barrett R.: Composition of light-duty  
367 motor vehicle exhaust particulate matter in the Denver, Colorado area. *Environ. Sci. Technol.*, 33:  
368 2328-2339, <https://doi.org/10.1021/es9810843>, 1999.

369 Cao, J., Wu, F., Chow, J., Lee, S., Li, Y., Chen, S., An, Z., Fung, K., Watson, J., and Zhu, C.:  
370 Characterization and source apportionment of atmospheric organic and elemental carbon during fall and  
371 winter of 2003 in Xi'an, China, *Atmos. Chem. Phys.*, 5, 3127-3137, [https://doi.  
372 org/10.5194/acp-5-3127-2005](https://doi.org/10.5194/acp-5-3127-2005), 2005.

373 Chen, H., Nanayakkara, C. E., and Grassian, V. H.: Titanium Dioxide Photocatalysis in Atmospheric  
374 Chemistry, *Chem. Rev.*, 112, 5919-5948, <https://doi.10.1021/cr3002092>, 2012.

375 Chow, J. C., Watson, J. G., Pritchett, L. C., Pierson, W. R., Frazier, C. A., and Purcell, R. G.: The dri  
376 thermal/optical reflectance carbon analysis system: description, evaluation and applications in U.S. Air  
377 quality studies, *Atmos. Environ., Part A. General Topics*, 27, 1185-1201,  
378 [https://doi.org/10.1016/0960-1686\(93\)90245-T](https://doi.org/10.1016/0960-1686(93)90245-T), 1993.

379 Chow, J. C., Watson, J. G., Chen, L. W. A., Chang, M. C. O., Robinson, N. F., Trimble, D., and Kohl, S.:  
380 The IMPROVE\_A Temperature Protocol for Thermal/Optical Carbon Analysis: Maintaining Consistency  
381 with a Long-Term Database, *J. Air Waste Manage.*, 57, 1014-1023,  
382 <https://doi.org/10.3155/1047-3289.57.9.1014>, 2007.

383 Chu, B., Wang, Y., Yang, W., Ma, J., Ma, Q., Zhang, P., Liu, Y., and He, H.: Effects of NO<sub>2</sub> and C<sub>3</sub>H<sub>6</sub>  
384 on the heterogeneous oxidation of SO<sub>2</sub> on TiO<sub>2</sub> in the presence or absence of UV irradiation, *Atmos.*  
385 *Chem. Phys. Discuss.*, 2019, 1-20, <https://doi.org/10.5194/acp-2019-532>, 2019.

386 Cong, Z., Kang, S., Kawamura, K., Liu, B., Wan, X., Wang, Z., Gao, S., and Fu, P.: Carbonaceous  
387 aerosols on the south edge of the Tibetan Plateau: concentrations, seasonality and sources, *Atmos. Chem.*  
388 *Phys.*, 15, 1573-1584, <https://doi.org/10.5194/acp-15-1573-2015>, 2015.

389 Cwiertny, D. M., Young, M. A., and Grassian, V. H.: Chemistry and photochemistry of mineral dust  
390 aerosol, *Annu. Rev. Phys. Chem.*, 59, 27-51, <https://doi.org/10.1146/annurev.physchem.59.032607.093630>, 2008.

392 Dai, W. T., Ho, S. S. H., Ho, K. F., Liu, W. D., Cao, J. J., and Lee, S. C.: Seasonal and diurnal variations  
393 of mono- and di-carbonyls in Xi'an, China, *Atmos. Res.*, 113, 102-112,  
394 <http://dx.doi.org/10.1016/j.atmosres.2012.05.001>, 2012.

395 Dentener, F. J., Carmichael, G. R., Zhang, Y., Lelieveld, J., and Crutzen, P. J.: Role of mineral aerosol as  
396 a reactive surface in the global troposphere, *J. Geophys. Res.-Atmos.*, 101, 22869-22889,  
397 <https://doi:10.1029/96JD01818>, 1996.

398 Dickerson, R. R., Kondragunta, S., Stenchikov, G., Civerolo, K. L., Doddridge, B. G., and Holben, B. N.:  
399 The Impact of Aerosols on Solar Ultraviolet Radiation and Photochemical Smog, *Science*, 278, 827,  
400 <https://doi:10.1126/science.278.5339.827>, 1997.

401 Duan, J., Guo, S., Tan, J., Wang, S., and Chai, F.: Characteristics of atmospheric carbonyls during haze  
402 days in Beijing, China, *Atmos. Res.*, 114, 17-27, <http://dx.doi.org/10.1016/j.atmosres.2012.05.010>, 2012.



403 Fan, R., Li, J., Chen, L., Xu, Z., He, D., Zhou, Y., Zhu, Y., Wei, F., and Li, J.: Biomass fuels and coke  
404 plants are important sources of human exposure to polycyclic aromatic hydrocarbons, benzene and  
405 toluene, *Environ. Res.*, 135, 1-8, <http://dx.doi.org/10.1016/j.envres.2014.08.021>, 2014.

406 Feng, T., Bei, N. F., Huang, R. J., Cao, J. J., Zhang, Q., Zhou, W. J., Tie, X. X., Liu, S. X., Zhang, T., Su,  
407 X. L., Lei, W. F., Molina, L. T., and Li, G. H.: Summertime ozone formation in Xi'an and surrounding  
408 areas, China, *Atmos. Chem. Phys.*, 16, 4323-4342, <http://doi.org/10.5194/acp-16-4323-2016>, 2016.

409 Ginoux, P., Chin, M., Tegen, I., Prospero, J. M., Holben, B., Dubovik, O., and Lin, S. J.: Sources and  
410 distributions of dust aerosols simulated with the GOCART model, *J. Geophys. Res.-Atmos.*, 106,  
411 20255-20273, <http://doi.10.1029/2000jd000053>, 2001.

412 Guo, S., Hu, M., Zamora, M. L., Peng, J. F., Shang, D. J., Zheng, J., Du, Z. F., Wu, Z., Shao, M., Zeng, L.  
413 M., Molina, M. J., and Zhang, R. Y.: Elucidating severe urban haze formation in China, *Proc. Natl. Acad.*  
414 *Sci. USA*, 111, 17373-17378, <https://doi.org/10.1073/pnas.1419604111>, 2014.

415 Guo, S., Hu, M., Lin, Y., Gomez-Hernandez, M., Zamora, M. L., Peng, J., Collins, D. R., and Zhang, R.:  
416 OH-Initiated Oxidation of m-Xylene on Black Carbon Aging, *Environ. Sci. Technol.*, 50, 8605-8612,  
417 <http://doi.org/10.1021/acs.est.6b01272>, 2016.

418 He, H., Wang, Y. S., Ma, Q. X., Ma, J. Z., Chu, B. W., Ji, D. S., Tang, G. Q., Liu, C., Zhang, H. X., and  
419 Hao, J. M.: Mineral dust and NO<sub>x</sub> promote the conversion of SO<sub>2</sub> to sulfate in heavy pollution days, *Sci.*  
420 *Rep.-UK.*, 4, <http://doi.10.1038/srep04172>, 2014.

421 Ho, K. F., Lee, S. C., Guo, H., and Tsai, W. Y.: Seasonal and diurnal variations of volatile organic  
422 compounds (VOCs) in the atmosphere of Hong Kong, *Sci. Total. Environ.*, 322, 155-166,  
423 <http://dx.doi.org/10.1016/j.scitotenv.2003.10.004>, 2004.

424 Ho, K. F., Lee, S. C., Ho, W. K., Blake, D. R., Cheng, Y., Li, Y. S., Ho, S. S. H., Fung, K., Louie, P. K.  
425 K., and Park, D.: Vehicular emission of volatile organic compounds (VOCs) from a tunnel study in Hong  
426 Kong, *Atmos. Chem. Phys.*, 9, 7491-7504, <http://doi.org/10.5194/acp-9-7491-2009>, 2009.

427 Ho, S. S. H., Ho, K. F., Liu, W. D., Lee, S. C., Dai, W. T., Cao, J. J., and Ip, H. S. S.: Unsuitability of  
428 using the DNPH-coated solid sorbent cartridge for determination of airborne unsaturated carbonyls,  
429 *Atmos. Environ.*, 45, 261-265, <http://doi.org/10.1016/j.atmosenv.2010.09.042>, 2011.

430 Ho, S. S. H., Chow, J. C., Watson, J. G., Wang, L., Qu, L., Dai, W., Huang, Y., and Cao, J.: Influences of  
431 relative humidities and temperatures on the collection of C<sub>2</sub>-C<sub>5</sub> aliphatic hydrocarbons with multi-bed

432 (Tenax TA, Carbograph 1TD, Carboxen 1003) sorbent tube method, *Atmos. Environ.*, 151, 45-51,  
433 <http://dx.doi.org/10.1016/j.atmosenv.2016.12.007>, 2017.

434 Ho, S. S. H., Wang, L., Chow, J. C., Watson, J. G., Xue, Y., Huang, Y., Qu, L., Li, B., Dai, W., Li, L.,  
435 and Cao, J.: Optimization and evaluation of multi-bed adsorbent tube method in collection of volatile  
436 organic compounds, *Atmos. Res.*, 202, 187-195, <https://doi.org/10.1016/j.atmosres.2017.11.026>, 2018.

437 Huang, R., Zhang, Y., Bozzetti, C., Ho, K., Cao, J., Han, Y., Daellenbach, K. R., Slowik, J. G., Platt, S.  
438 M., Canonaco, F., Zotter, P., Wolf, R., Pieber, S. M., Brun, E. A., Crippa, M., Ciarelli, G., Piazzalunga,  
439 A., Schwikowski, M., Abbaszade, G., Schnelle-Kreis, J., Zimmermann, R., An, Z., Szidat, S.,  
440 Baltensperger, U., Haddad, I. E., and Prevot, A. S. H.: High secondary aerosol contribution to particulate  
441 pollution during haze events in China, *Nature*, 514, 218-222, <https://doi.org/10.1038/nature13774>, 2014.

442 Huang X, Yu J, He L, Hu M.: Size distribution characteristics of elemental carbon emitted from Chinese  
443 vehicles: Results of a tunnel study and atmospheric implications. *Environ. Sci. Technol.*, 40: 5355-5360,  
444 <https://doi.org/10.1021/es0607281>, 2006.

445 Huang, Y., Ling, Z. H., Lee, S. C., Ho, S. S. H., Cao, J. J., Blake, D. R., Cheng, Y., Lai, S. C., Ho, K. F.,  
446 Gao, Y., Cui, L., and Louie, P. K. K.: Characterization of volatile organic compounds at a roadside  
447 environment in Hong Kong: An investigation of influences after air pollution control strategies, *Atmos.*  
448 *Environ.*, 122, 809-818, <http://dx.doi.org/10.1016/j.atmosenv.2015.09.036>, 2015.

449 Li, B., Ho, S. S. H., Xue, Y., Huang, Y., Wang, L., Cheng, Y., Dai, W., Zhong, H., Cao, J., and Lee, S.:  
450 Characterizations of volatile organic compounds (VOCs) from vehicular emissions at roadside  
451 environment: The first comprehensive study in Northwestern China, *Atmos. Environ.*, 161, 1-12,  
452 <https://doi.org/10.1016/j.atmosenv.2017.04.029>, 2017.

453 Liu, W., Zhang, J., Kwon, J., Weisel, C., Turpin, B., Zhang, L., Korn, L., Morandi, M., Stock, T., and  
454 Colome, S.: Concentrations and Source Characteristics of Airborne Carbonyl Compounds Measured  
455 Outside Urban Residences, *J. Air Waste Manage.*, 56, 1196-1204,  
456 <https://doi.org/10.1080/10473289.2006.10464539>, 2006.

457 Liu, Y., Shao, M., Fu, L., Lu, S., Zeng, L., and Tang, D.: Source profiles of volatile organic compounds  
458 (VOCs) measured in China: Part I, *Atmos. Environ.*, 42, 6247-6260,  
459 <http://dx.doi.org/10.1016/j.atmosenv.2008.01.070>, 2008a.

460 Liu, Y., Shao, M., Lu, S., Chang, C.-C., Wang, J.-L., and Fu, L.: Source apportionment of ambient  
461 volatile organic compounds in the Pearl River Delta, China: Part II, *Atmos. Environ.*, 42, 6261-6274,  
462 <https://doi.org/10.1016/j.atmosenv.2008.02.027>, 2008b.

463 Ndour, M., Conchon, P., D'Anna, B., Ka, O., and George, C.: Photochemistry of mineral dust surface as  
464 a potential atmospheric renoxification process, *Geophys. Res. Lett.*, 36, 4,  
465 <https://doi.org/10.1029/2008gl036662>, 2009.

466 Ni, H., Huang, R., Cao, J., Liu, W., Zhang, T., Wang, M., Meijer, H. A. J., and Dusek, U.: Source  
467 apportionment of carbonaceous aerosols in Xi'an, China: insights from a full year of measurements of  
468 radiocarbon and the stable isotope C-13, *Atmos. Chem. Phys.*, 18, 16363-16383,  
469 <https://doi.org/10.5194/acp-18-16363-2018>, 2018

470 Nie, W., Ding, A. J., Wang, T., Kerminen, V. M., George, C., Xue, L. K., Wang, W. X., Zhang, Q. Z.,  
471 Petaja, T., Qi, X. M., Gao, X. M., Wang, X. F., Yang, X. Q., Fu, C. B., and Kulmala, M.: Polluted dust  
472 promotes new particle formation and growth, *Sci. Rep.-UK.*, 4, 6, <https://doi.org/10.1038/srep06634>,  
473 2014.

474 Perring, A. E., Pusede, S. E., and Cohen, R. C.: An Observational Perspective on the Atmospheric  
475 Impacts of Alkyl and Multifunctional Nitrates on Ozone and Secondary Organic Aerosol, *Chem. Rev.*,  
476 113, 5848-5870, <https://doi.org/10.1021/cr300520x>, 2013.

477 Shao, M., Lu, S. H., Liu, Y., Xie, X., Chang, C. C., Huang, S., and Chen, Z. M.: Volatile organic  
478 compounds measured in summer in Beijing and their role in ground-level ozone formation, *J. Geophys.*  
479 *Res.-Atmos.*, 114, D00G06, <https://doi.org/10.1029/2008jd010863>, 2009.

480 Song, S. J., Gao, M., Xu, W. Q., Sun, Y. L., Worsnop, D. R., Jayne, J. T., Zhang, Y. Z., Zhu, L., Li, M.,  
481 Zhou, Z., Cheng, C. L., Lv, Y. B., Wang, Y., Peng, W., Xu, X. B., Lin, N., Wang, Y. X., Wang, S. X.,  
482 Munger, J. W., Jacob, D. J., and McElroy, M. B.: Possible heterogeneous chemistry of  
483 hydroxymethanesulfonate (HMS) in northern China winter haze, *Atmos. Chem. Phys.*, 19, 1357-1371,  
484 <https://doi.org/10.5194/acp-19-1357-2019>, 2019.

485 Tao J, Zhang Z, Wu Y, Zhang L, Wu Z, Cheng P.: Impact of particle number and mass size distributions  
486 of major chemical components on particle mass scattering efficiency in urban Guangzhou in southern  
487 China. *Atmos. Chem. Phys.*, 19, 8471-8490, <https://doi.org/10.1021/es9810843>, 2019

488 Warneke, C., de Gouw, J. A., Edwards, P. M., Holloway, J. S., Gilman, J. B., Kuster, W. C., Graus, M.,  
489 Atlas, E., Blake, D., Gentner, D. R., Goldstein, A. H., Harley, R. A., Alvarez, S., Rappenglueck, B.,

490 Trainer, M., and Parrish, D. D.: Photochemical aging of volatile organic compounds in the Los Angeles  
491 basin: Weekday-weekend effect, *J. Geophys. Res.-Atmos.*, 118, 5018-5028,  
492 <http://doi.org/10.1002/jgrd.50423>, 2013.

493 Wu, F., Chow, J. C., An, Z., Watson, J. G., and Cao, J.: Size-Differentiated Chemical Characteristics of  
494 Asian Paleo Dust: Records from Aeolian Deposition on Chinese Loess Plateau, *J. Air Waste Manage.*, 61,  
495 180-189, 10.3155/1047-3289.61.2.180, 2011.

496 Xu, H., Cao, J., Chow, J. C., Huang, R. J., Shen, Z., Chen, L. W. A., Ho, K. F., and Watson, J. G.:  
497 Inter-annual variability of wintertime PM<sub>2.5</sub> chemical composition in Xi'an, China: Evidences of  
498 changing source emissions, *Sci. Total. Environ.*, 545, 546-555,  
499 <http://dx.doi.org/10.1016/j.scitotenv.2015.12.070>, 2016.

500 Xue, L., Wang, T., Louie, P. K. K., Luk, C. W. Y., Blake, D. R., and Xu, Z.: Increasing External Effects  
501 Negate Local Efforts to Control Ozone Air Pollution: A Case Study of Hong Kong and Implications for  
502 Other Chinese Cities, *Environ. Sci. Technol.*, 48, 10769-10775, 10.1021/es503278g, 2014.

503 Xue, L. K., Wang, T., Guo, H., Blake, D. R., Tang, J., Zhang, X. C., Saunders, S. M., and Wang, W. X.:  
504 Sources and photochemistry of volatile organic compounds in the remote atmosphere of western China:  
505 results from the Mt. Waliguan Observatory, *Atmos. Chem. Phys.*, 13, 8551-8567,  
506 10.5194/acp-13-8551-2013, 2013.

507 Xue, Y., Ho, S. S. H., Huang, Y., Li, B., Wang, L., Dai, W., Cao, J., and Lee, S.: Source apportionment  
508 of VOCs and their impacts on surface ozone in an industry city of Baoji, Northwestern China, *Sci.*  
509 *Rep.-UK.*, 7, 9979, <https://doi.org/10.1038/s41598-017-10631-4>, 2017.

510 Zhang, D. Z., Shi, G. Y., Iwasaka, Y., and Hu, M.: Mixture of sulfate and nitrate in coastal atmospheric  
511 aerosols: individual particle studies in Qingdao (36 degrees 04 ' N, 120 degrees 21 ' E), China, *Atmos.*  
512 *Environ.*, 34, 2669-2679, [http://doi.org/10.1016/s1352-2310\(00\)00078-9](http://doi.org/10.1016/s1352-2310(00)00078-9), 2000.

513 Zhang, D. Z., Zang, J. Y., Shi, G. Y., Iwasaka, Y., Matsuki, A., and Trochkin, D.: Mixture state of  
514 individual Asian dust particles at a coastal site of Qingdao, China, *Atmos. Environ.*, 37, 3895-3901,  
515 [http://doi.org/10.1016/s1352-2310\(03\)00506-5](http://doi.org/10.1016/s1352-2310(03)00506-5), 2003.

516 Zhang, N., Cao, J., Wang, Q., Huang, R., Zhu, C., Xiao, S., and Wang, L.: Biomass burning influences  
517 determination based on PM<sub>2.5</sub> chemical composition combined with fire counts at southeastern Tibetan  
518 Plateau during pre-monsoon period, *Atmos. Res.*, 206, 108-116,  
519 <https://doi.org/10.1016/j.atmosres.2018.02.018>, 2018.

520 Zhang, Q., Shen, Z., Cao, J., Zhang, R., Zhang, L., Huang, R. J., Zheng, C., Wang, L., Liu, S., Xu, H.,  
521 Zheng, C., and Liu, P.: Variations in PM<sub>2.5</sub>, TSP, BC, and trace gases (NO<sub>2</sub>, SO<sub>2</sub>, and O<sub>3</sub>) between  
522 haze and non-haze episodes in winter over Xi'an, China, *Atmos. Environ.*, 112, 64-71,  
523 <https://doi.org/10.1016/j.atmosenv.2015.04.033>, 2015a.

524 Zhang, T., Cao, J. J., Tie, X. X., Shen, Z. X., Liu, S. X., Ding, H., Han, Y. M., Wang, G. H., Ho, K. F.,  
525 Qiang, J., and Li, W. T.: Water-soluble ions in atmospheric aerosols measured in Xi'an, China: Seasonal  
526 variations and sources, *Atmos. Res.*, 102, 110-119, <https://doi.org/10.1016/j.atmosres.2011.06.014>, 2011.

527 Zhang, Y., Wang, X., Zhang, Z., Lu, S., Huang, Z., and Li, L.: Sources of C<sub>2</sub>-C<sub>4</sub> alkenes, the most  
528 important ozone nonmethane hydrocarbon precursors in the Pearl River Delta region, *Sci. Total Environ.*,  
529 502, 236-245, <https://doi.10.1016/j.scitotenv.2014.09.024>, 2015b.

530 Zhang, Y., Bao, F., Li, M., Chen, C., and Zhao, J.: Nitrate-Enhanced Oxidation of SO<sub>2</sub> on Mineral Dust:  
531 A Vital Role of a Proton, *Environ. Sci. Technol.*, 53, 10139-10145, <https://doi.10.1021/acs.est.9b01921>,  
532 2019.

533 Zhang, Z., Wang, X., Zhang, Y., Lü, S., Huang, Z., Huang, X., and Wang, Y.: Ambient air benzene at  
534 background sites in China's most developed coastal regions: Exposure levels, source implications and  
535 health risks, *Sci. Total Environ.*, 511, 792-800, <http://dx.doi.org/10.1016/j.scitotenv.2015.01.003>, 2015c.

536 Zheng Fang, W. D., Yanli Zhang, Xiang Ding, Mingjin Tang, Tengyu Liu, Qihou Hu, Ming Zhu, Zhaoyi  
537 Wang, Weiqiang Yang, Zhonghui Huang, Wei Song, Xinhui Bi, Jianmin Chen, Yele Sun, Christian  
538 George, and Xinming Wang: Open burning of rice, corn and wheat straws: primary emissions,  
539 photochemical aging, and secondary organic aerosol formation, *Atmos. Chem. Phys.*, 17, 14821-14839,  
540 <http://org/10.5194/acp-17-14821-2017>, 2017.

541 Zou, Y., Deng, X., Zhu, D., Gong, D., Wang, H., Li, F., Tan, H., Deng, T., Mai, B., and Liu, X.:  
542 Characteristics of 1 year of observational data of VOCs, NO<sub>x</sub> and O<sub>3</sub> at a suburban site in Guangzhou,  
543 China, *Atmos. Chem. Phys.*, 15, 6625-6636, <https://doi.org/10.5194/acp-15-6625-2015>, 2015.

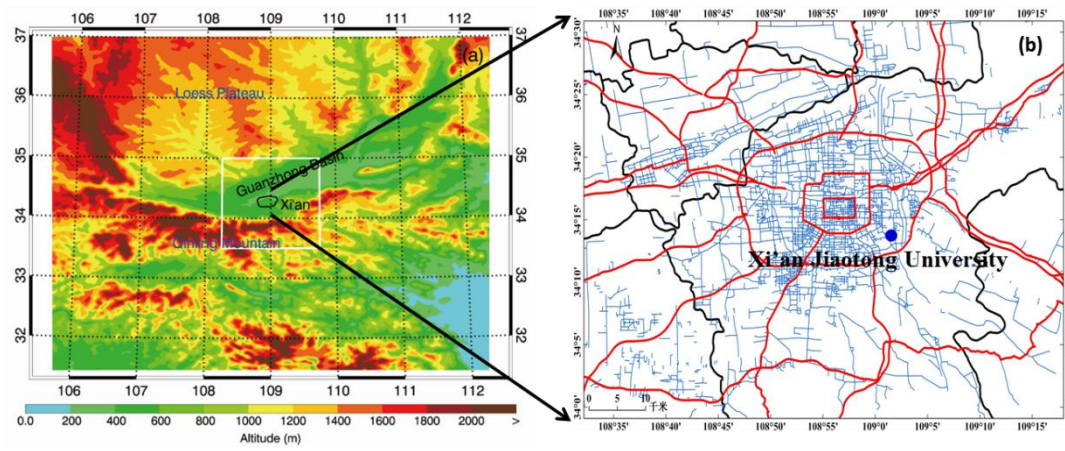
544



545

546

547  
548



549

550 **Figure 1: Regional and local maps of the study area, (a) Regional map showing the location of Xi'an and the**  
551 **surrounding geography; (b) local map of Xi'an showing the sampling site (blue dot), main roads (red lines),**  
552 **and secondary roads (blue lines).**

553

554

555

556

557

558

559

560

561

562

563

564

565

566

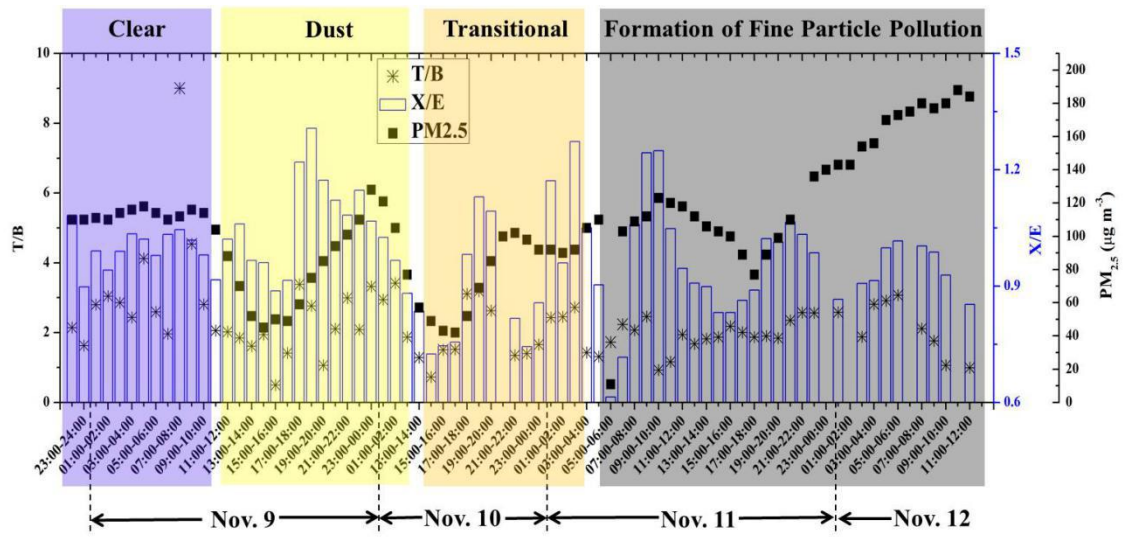
567

568

569

570

571



572

573 Figure 2: Variations in the ratios of indicator volatile organic compound (VOC) species (toluene/benzene  
574 [T/B], and m-,p-xylene/ethylbenzene [X/E]) and fine particle loadings during the study period.

575

576

577

578

579

580

581

582

583

584

585

586

587

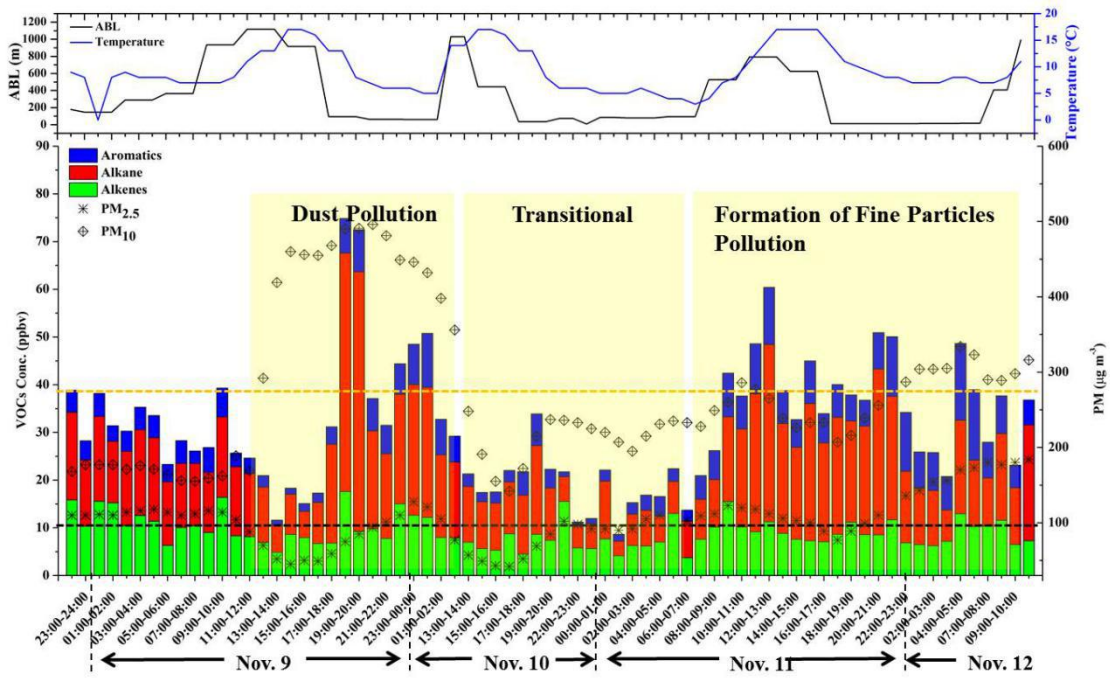
588

589

590

591

592



593

594 Figure 3: Temporal variations in volatile organic compound (VOC) concentrations and particle levels during  
595 the sampling period (9–13 November 2016).

596

597

598

599

600

601

602

603

604

605

606

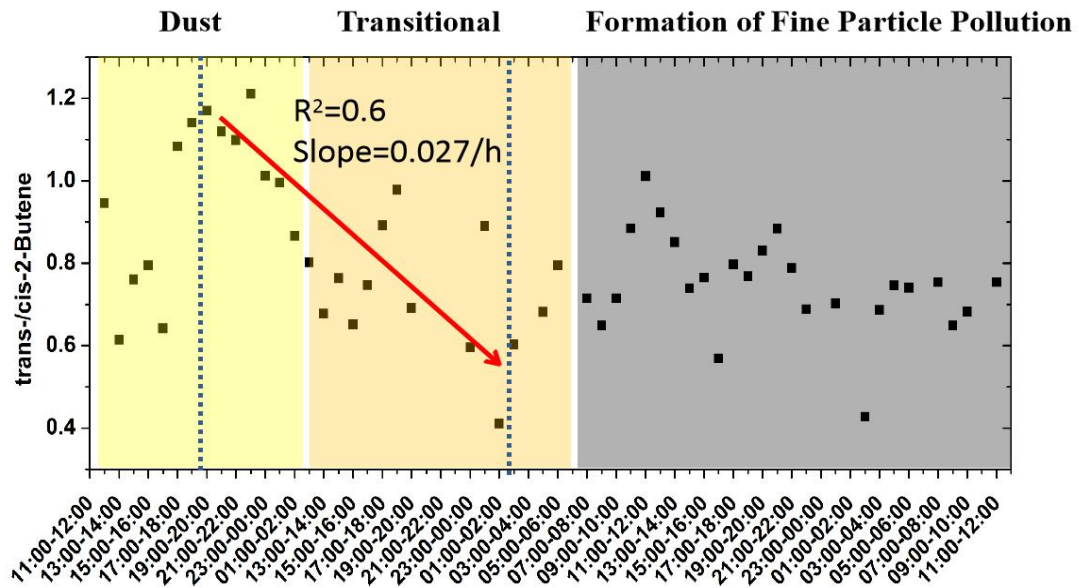
607

608

609



610  
611  
612

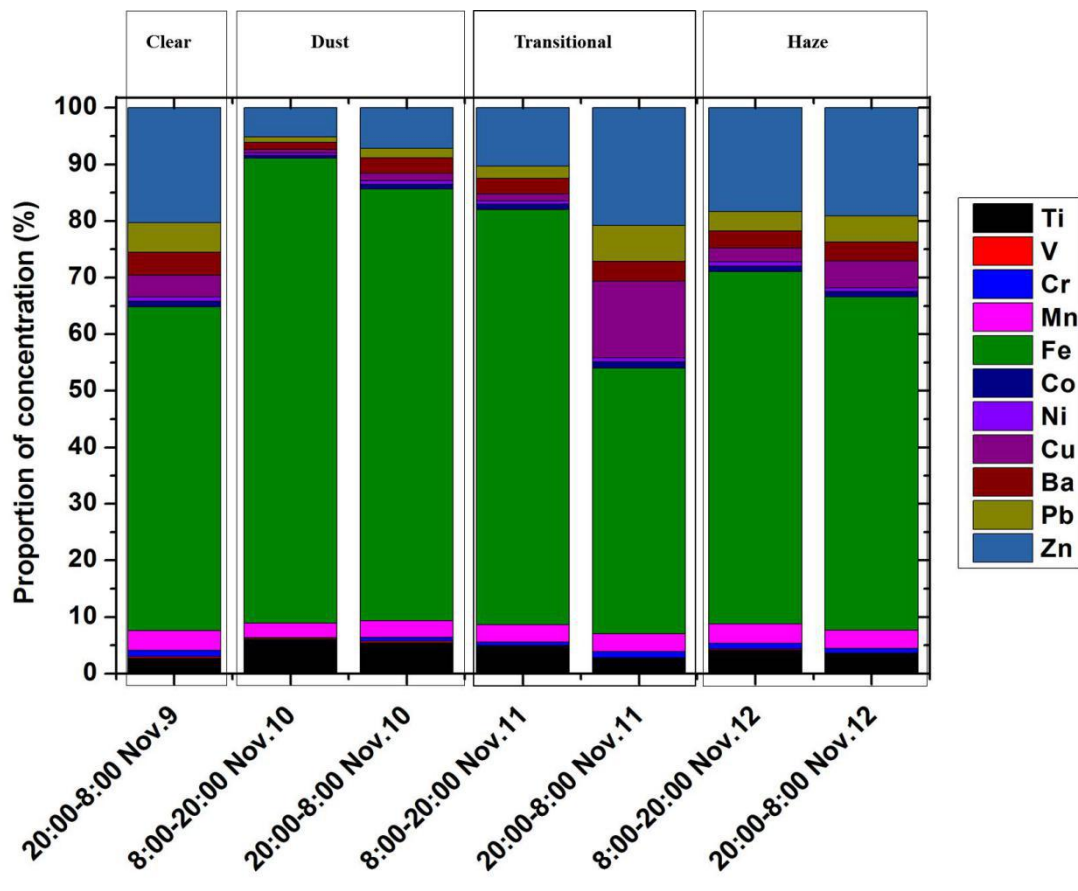


613

614 Figure 4: Temporal variation of trans-/cis-2-butene ratio in the dust-transitional-fine particle pollution  
615 period.

616  
617  
618  
619  
620  
621  
622  
623  
624  
625  
626  
627  
628  
629

630  
631  
632  
633  
634



635

636 Figure 5: Composition of selected metallic elements in the PM2.5 samples.

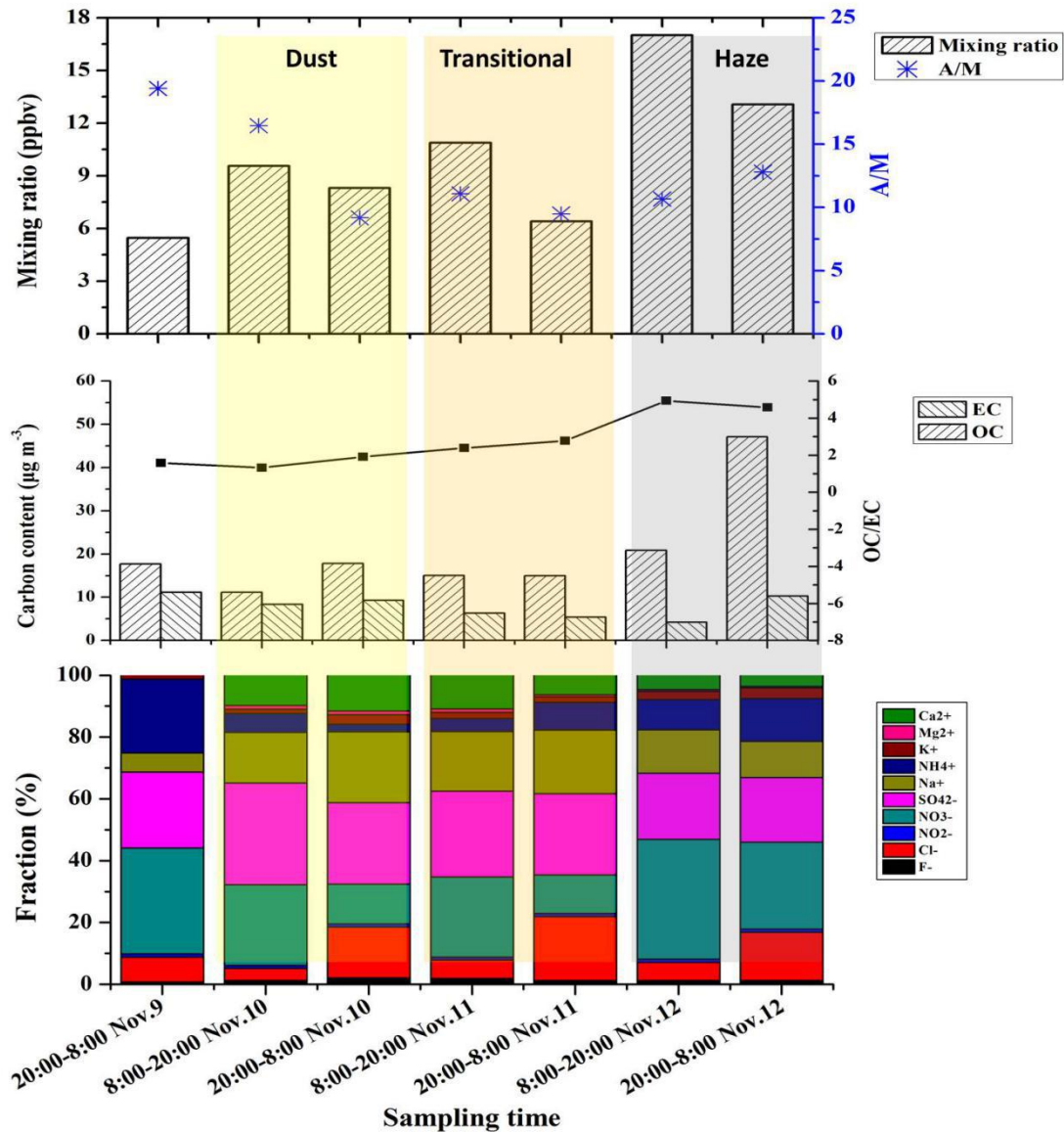
637  
638  
639  
640  
641  
642  
643  
644

645

646

647

648



649

650 **Figure 6: Variations in (a) the mixing ratios of 17 carbonyl compounds and acetone to methylglyoxal (A/M)**  
651 **ratios in the gas phase, (b) particulate carbon fractions, (c) and particulate water-soluble ions during the**  
652 **study period.**

653

654

655